ON GENERALIZED FRACTIONAL PROCESSES

by

Henry L. Gray, Nien-Fan Zhang, Wayne A. Woodward

Technical Report No. SMU/DS/TR/223
Department of Statistical Science

August 1988

Department of Statistical Science
Southern Methodist University
Dallas, Texas 75275

ON GENERALIZED FRACTIONAL PROCESSES

by

Henry L. Gray, Nien Fan Zhang, Wayne A. Woodward
Department of Statistical Science
Southern Methodist University
Dallas, Texas 75275

ABSTRACT

A class of stationary, long memory processes is proposed which is an extension of the fractional autoregressive moving average (FARMA) model. The FARMA model is limited by the fact that it does not allow data with persistent cyclic (or seasonal) behavior to be considered. Our extension, which includes the FARMA model as a special case, makes use of the properties of the generating function of the Gegenbauer polynomials, and we refer to these models as Gegenbauer autoregressive moving average (GARMA) models. While the FARMA model has a peak in the spectrum at f=0, the GARMA process can model long term periodic behavior for any frequency $0 \leq f \leq .5$. Properties of the GARMA process are examined and techniques for generation of realizations, model identification and parameter estimation are proposed. The use of the GARMA model is illustrated through simulated examples as well as with the classical sunspot data.

Key Words: Time series, long memory, stationary process, fractional difference, FARMA model, Gegenbauer polynomials, GARMA model.

On Generalized Fractional Processes

by

H. L. Gray, Nien Fan Zhang, Wayne A. Woodward

Southern Methodist University

1. Introduction

In recent years much attention has been focused on the study of "long memory processes". A stationary time series defined over $t = 0, \pm 1, \pm 2, \ldots$ is said to be long memory if $\Sigma_{k=0}^{\infty} |\gamma(k)|$ diverges, where $\gamma(k)$ is the autocovariance of the process. Otherwise the time series is called a short memory process. See McLeod and Hipel (1978). An essentially equivalent definition of long memory in terms of the power spectrum is given in Definition 1 which is a slight extension of previous definitions.

Definition 1. A discrete time series is said to be long memory if for some $\omega \varepsilon [0,\pi]$ the power spectrum, $P(\omega)$, becomes unbounded.

Currently the most popular technique for analyzing long memory time series is through the so called fractional difference, ∇^{λ}, where

$$\nabla^{\lambda} f(t) = (1-B)^{\lambda} f(t) = \sum_{k=0}^{\infty} (-1)^k \binom{\lambda}{k} B^k f(t)$$

$$= \sum_{k=0}^{\infty} (-1)^k \binom{\lambda}{k} f(t-k) \quad , \qquad (1)$$

since $B^k f(t) = f(t-k)$.

Using the definition in (1), Hosking (1981, 1984), Granger and Joyeux (1980) and Geweke and Porter-Hudak (1983) have posed the fractional autoregressive-moving average (FARMA) process as a model for long memory data. A process is called a FARMA process if

$$\phi(B)(1-B)^d(X(t)-\mu) = \theta(B)a(t), \tag{2}$$

where a(t) is white noise and

$$\begin{aligned} B^k X(t) &= X(t-k) \\ \phi(B) &= 1-\phi_1 B - \phi_2 B^2 - \ldots - \phi_p B^p \\ \theta(B) &= 1-\theta_1 B - \theta_2 B^2 - \ldots - \theta_q B^q \ . \end{aligned} \tag{3}$$

If $\phi(B)$ is a stationary operator and $d < 1/2$, then it can be shown that X(t) in (2) is a stationary process. If also $d > 0$, then X(t) is long memory with an autocorrelation that is asymptotically equivalent to τ^{2d-1} as $\tau \to \infty$, i.e. $\rho(\tau) \simeq \tau^{2d-1}$ as $\tau\to\infty$. We will say $f(\tau) \simeq g(\tau)$ as $\tau\to\infty$ if $\lim_{\tau\to\infty} [f(\tau)/g(\tau)] = c$ where c is a finite, nonzero constant. Moreover in this event $P(\omega) \simeq \omega^{-2d}$ as $\omega\to 0$. See Hosking (1981).

Even though a significant amount of work has been done making use of the model in (2), it is doubtful that the FARMA model will furnish a sufficiently broad base to address the long memory problem in general without some significant extensions to the model in (2). Some extensions have been suggested already. For example, Hosking (1981, 1984) suggested the model

$$\phi(B)(1-2uB + B^2)^{\lambda}(X(t)-\mu) = \theta(B)a(t) \quad , \tag{4}$$

which clearly includes (2) and would allow long memory seasonal behavior. This model however has not been investigated, presumably due to the complexity in inverting the factor $(1-2uB + B^2)^{\lambda}$.

In this paper we show how the fractional model can be extended to include the factor $(1-2uB + B^2)^{\lambda}$. This is accomplished by making use of the generating function of the Gegenbauer polynomials. The resulting linear processes are much more general than the fractional model produces and they allow one to consider long term periodicitities in the data.

2. Gegenbauer Polynomials

The Gegenbauer polynomials have a rich history in applied mathematics due primarily to their orthogonality and recursion properties. In this paper, however, it is neither of these properties that we exploit but instead we make use of their generating function.

Although one can define these polynomials directly it is not uncommon to define them through their generating function as we shall do now. See Magnus, Oberhettinger and Soni (1966) or Rainville (1960).

Definition 2. Let $\lambda \neq 0$ and $|Z| < 1$, then for $|u| \leq 1$ we define the Gegenbauer polynomials, $C_n^{(\lambda)}(u)$, by

$$(1-2uZ + Z^2)^{-\lambda} = \sum_{n=0}^{\infty} C_n^{(\lambda)}(u)Z^n \quad . \tag{5}$$

As stated previously, these polynomials can be defined directly. Even though we will have no need for their definition apart from Equation (5), for completeness we state the following result. From

(5) it can be shown that (see Rainville (1960))

$$C_n^{(\lambda)}(u) = \sum_{k=0}^{[n/2]} \frac{(-1)^k(\lambda)_{n-k}(2u)^{n-2k}}{k!(n-2k)!} \tag{6}$$

where $(\alpha)_n = \frac{\Gamma(\alpha+n)}{\Gamma(\alpha)}$.

3. The Gegenbauer Process

Let $C_k^{(\lambda)}(u)$ be the Gegenbauer polynomial defined in Definition 2 and let X(t) to be the general linear process given by

$$X(t) - \mu = \sum_{k=0}^{\infty} C_k^{(\lambda)}(u)a(t-k), \quad t = 0, \pm 1, \pm 2, \ldots, \tag{7}$$

where a(t) is white noise with mean zero and variance σ_a^2 and λ is any real number $\neq 0$. In the remainder of this section we will assume without loss of generality that $\mu = 0$.

Note that from (5) and (7) we can rewrite X(t) as

$$\begin{aligned} X(t) &= \sum_{k=0}^{\infty} C_k^{(\lambda)}(u)B^k a(t) \\ &= (1-2uB + B^2)^{-\lambda} a(t) , \end{aligned} \tag{8}$$

and also if X(t) is invertible, we can formally write

$$(1-2uB + B^2)^{\lambda} X(t) = a(t) . \tag{9}$$

Invertibility conditions for X(t) are given in Theorem 1. We thus have the following definition.

Definition 3. The discrete process X(t) given in (7) is called a Gegenbauer process with parameters u and λ and will typically be

denoted using the notation in (9).

It should be noted that if $u = 1$, we have

$$(1-B)^{2\lambda}X(t) = a(t) \tag{10}$$

so that $X(t)$ is just the standard fractional process of order 2λ while if $u = -1$, (9) becomes

$$(1+B)^{2\lambda}X(t) = a(t) \ . \tag{11}$$

Note that when $u=1$, the name "fractional difference" seems appropriate but for $u \neq 1$ there is no such interpretation. On the other hand, the process is Gegenbauer for all u.

In Theorem 1 which follows we provide stationarity and invertibility conditions while in Theorem 2 we establish the long memory behavior of a Gegenbauer process.

<u>Theorem 1</u>. (a) A Gegenbauer process is stationary

i) if $|u| < 1$ and $\lambda < 1/2$

ii) if $u = \pm 1$ and $\lambda < 1/4$.

(b) A Gegenbauer process is invertible

i) if $|u| < 1$ and $\lambda > -1/2$

ii) if $u = \pm 1$ and $\lambda > -1/4$.

Proof: a(i) Suppose $|u| < 1$. Then

$$C_k^{(\lambda)}(u) = \frac{\Gamma(\lambda+\frac{1}{2})\Gamma(2\lambda+k)}{k!\Gamma(2\lambda)} \left(\frac{1-u^2}{4}\right)^{\frac{1}{4}-\frac{\lambda}{2}} P_{k+\lambda-\frac{1}{2}}^{(\frac{1}{2}-\lambda)}(u) \quad ,$$

where $P_k^{(\lambda)}(u)$ is the Legendre function of the first kind.

See Magnus, Oberhettinger and Soni (1966), page 219. Now for fixed u and η, as $\mathrm{Re}(\alpha)\to\infty$ the following asymptotic result holds when $|u| < 1$.

$$P_\alpha^\eta(u) = \frac{2\,\Gamma(\alpha+\eta+1)}{\sqrt{\pi}\,\Gamma(\alpha+3/2)}\,\frac{\cos[(\alpha+\frac{1}{2})\phi - \pi/4 + \eta\pi/2]}{(2\sin\phi)^{\frac{1}{2}}}[1 + O(1/\alpha)] ,$$

where $\phi = \cos^{-1}u$. Then

$$P_{(k+\lambda-\frac{1}{2})}^{(\frac{1}{2}-\lambda)}(u) = \frac{2}{\sqrt{\pi}}\,\frac{\Gamma(k+1)}{\Gamma(k+\lambda+1)}\,\frac{\cos[(k+\lambda)\phi-\lambda\pi/2]}{(2\sin\phi)^{\frac{1}{2}}}\,[1 + O(1/k)] . \qquad (12)$$

Therefore

$$C_k^{(\lambda)}(u) = \frac{2\Gamma(\lambda + \frac{1}{2})}{\sqrt{\pi}\,\Gamma(k+\lambda+1)}\,\frac{\Gamma(2\lambda+k)}{\Gamma(2\lambda)}\left(\frac{1-u^2}{4}\right)^{1/4-\lambda/2}$$

$$\bullet\ \frac{\cos[(k+\lambda)\phi - \lambda\pi/2]}{(2\sin\phi)^{\frac{1}{2}}}\,[1 + O(1/k)] .$$

Then by Sterling's formula

$$C_k^{(\lambda)}(u) \simeq \frac{2}{\sqrt{\pi}}\,\frac{\Gamma(\lambda + \frac{1}{2})}{\Gamma(2\lambda)}\left(\frac{1-u^2}{4}\right)^{\frac{1}{4}-\frac{\lambda}{2}}\cos[(k+\lambda)\phi - \frac{\lambda\pi}{2}]k^{\lambda-1} \qquad (13)$$

as $k \to \infty$.

Now

$$\gamma(0) = \sum_{k=0}^{\infty}[C_k^{(\lambda)}(u)]^2\sigma_a^2 . \qquad (14)$$

But from (13), when $|u| < 1$, the series in (14) converges if $\lambda < \frac{1}{2}$, which completes the proof for the case $|u| < 1$.

a(ii) The case u=1 was shown by Hosking (1981) and u=-1 follows similarly.

(b) From the proof of (a) it can be seen that X(t) in (7) can be written in the form

$$X(t) = a(t) - \sum_{k=1}^{\infty} C_k^{(-\lambda)}(u)X(t-k) \tag{15}$$

if $|u| < 1$ and $\lambda > -1/2$ or if $\lambda > -1/4$ when $u = \pm 1$, and thus the result follows.

<u>Theorem 2</u>. A stationary Gegenbauer process is long memory if $0<\lambda<\frac{1}{2}$ and $|u| < 1$ or if $|u| = 1$ and $0 < \lambda < 1/4$.

Proof: From (8), the spectrum, P(f) is given by

$$\begin{aligned} P(\omega) &= \sigma_a^2 \left| 1-2ue^{i\omega} + e^{2i\omega} \right|^{-2\lambda} \\ &= \sigma_a^2 \left[4(\cos\omega - u)^2\right]^{-\lambda} \quad . \end{aligned} \tag{16}$$

Then when $\omega = \cos^{-1}u$ the spectrum becomes unbounded, i.e. the covariance is not absolutely summable, and hence the process is long memory. The frequency $\omega_0 = \cos^{-1}u$ will be referred to as the Gegenbauer frequency (G-frequency). When $|u| = 1$, the results follow from Hosking (1981).

In Figure 1 we show the range of u and λ associated with stationary, long memory Gegenbauer processes. These u and λ values are associated with the shaded region, i.e. $0 < \lambda < .5$ and $|u| < 1$ as well as with the u,λ values along the solid horizontal line segments where $u = \pm 1$ and $0<\lambda<.25$. The fractional process of Hosking is represented by the solid horizontal line segment at the top of the

rectangle in Figure 1 from (0,1) to (.25,1) in the u,λ plane. This figure illustrates the fact that the Gegenbauer process is a substantial extension of the fractional process. As u and λ move along a path toward the boundary of the rectangle, the corresponding Gegenbauer processes approach nonstationarity if the path terminates somewhere along the dotted boundary. For example, if λ is held constant at $\lambda = .3$, then as u approaches 1 from below, the processes associated with these u and λ values will progressively exhibit more "near nonstationary" behavior. Thus it is clear that while u plays a role of determining the Gegenbauer frequency, it also is involved in the degree of "near nonstationarity" displayed by the model.

Note that when $u = 1$, the spectrum in (16) is the spectrum of the fractional process given by Hosking (1981). As has already been mentioned, in the case $u = 1$ it has been shown by Hosking (1981) that $\rho(\tau) \simeq \tau^{4\lambda-1}$ as $\tau \to \infty$. In the following theorem we show that for a Gegenbauer process, $\rho(\tau) \simeq \tau^{2\lambda-1}\sin(\pi\lambda-2\pi k f_0)$ where f_0 is the G-frequency.

In the proof of Theorem 3 we will make use of the concept of a slowly varying function.

<u>Definition 4</u>: A function $b(\omega)$ is said to be slowly varying at ω_0 if for $\delta > 0$, the following two conditions hold:

(a) $(\omega-\omega_0)^{\delta}b(\omega)$ is increasing and

$(\omega-\omega_0)^{-\delta}b(\omega)$ is decreasing

in some right hand neighborhood of ω_0

(b) $(\omega_0-\omega)^{\delta}b(\omega)$ is decreasing and

$(\omega_0-\omega)^{-\delta}b(\omega)$ is increasing in some left hand neighborhood of ω_0.

A function is said to be slowly varying from the right if (a) holds.

<u>Theorem 3</u>. Let $\{X(t)\}$ be a stationary, long memory Gegenbauer process, i.e.

$$(1-2uB+B^2)^{\lambda}X(t) = a(t) .$$

(a) When u=1 and $0 < \lambda < 1/4$, the autocorrelation function of $\{X(t)\}$ is

$$\rho(\tau) = \frac{\Gamma(1-2\lambda)\Gamma(\tau+2\lambda)}{\Gamma(2\lambda)\Gamma(\tau-2\lambda+1)} .$$

As $\tau \to \infty$, $\rho(\tau) \simeq \tau^{4\lambda-1}$.

(b) When u=-1 and $0<\lambda<1/4$, the autocorrelation function of $\{X(t)\}$ is

$$\rho(\tau) = (-1)^{\tau} \frac{\Gamma(1-2\lambda)\Gamma(\tau+2\lambda)}{\Gamma(2\lambda)\Gamma(\tau-2\lambda+1)} .$$

As $\tau \to \infty$, $\rho(\tau) \simeq (-1)^{\tau}\tau^{4\lambda-1}$.

(c) When $|u| < 1$ and $0<\lambda<1/2$,

$$\rho(\tau) \simeq \tau^{2\lambda-1}\sin(\pi\lambda - \tau\omega_0)$$

as $\tau\to\infty$ where ω_0 is the G-frequency.

Proof:

(a) Since the case u=1 is the fractional process, the result was shown by Hosking (1981).

(b) When $u = -1$, (9) becomes $(1+B)^{2\lambda}X(t)=a(t)$, i.e. $X(t) = (1+B)^{-2\lambda}a(t)$. The ψ weights in the general linear process form $X(t) = \Sigma_{k=0}^{\infty}\psi(k)a(t-k)$ can be written as

$$\psi(k) = (-1)^k \frac{\Gamma(k+2\lambda)}{k!\Gamma(2\lambda)}$$

$$= (-1)^k\eta(k)$$

where $\eta(k)$ are the ψ-weights found by Hosking (1981) in the case $u=1$ and the result follows by the proof of Hosking.

(c) We need the following lemma.

<u>Lemma</u>: Let $R(\tau) = \int_0^{\pi}P(\omega) \cos(\tau\omega)d\omega$ with τ an integer. Let $\omega_0 \in (0,\pi)$ and suppose $P(\omega)$ can be expressed as

$$P(\omega) = b(\omega) \mid \omega - \omega_0 \mid^{-\beta} \quad \text{with } 0 < \beta < 1/2 .$$

Further, suppose that $b(\omega)$ is non-negative and of bounded variation in $(0,\omega_0-\varepsilon) \cup (\omega_0+\varepsilon,\pi)$ for $\varepsilon>0$. Suppose also that $b(\omega)$ is slowly varying at ω_0. Then, when $\tau \to \infty$,

$$R(\tau) \simeq \tau^{\beta-1} \sin\left(\frac{\pi\beta}{2} - \tau\omega_0\right)\left[b_1\left(\frac{1}{\tau}\right) + b_2\left(\frac{1}{\tau}\right)\right]$$

with $b_1(x) = b(x+\omega_0)$ and $b_2(x) = b_1(-x)$.

Proof of Lemma: Consider

$$R(\tau) = \int_0^{\pi} b(\omega) \mid \omega - \omega_0 \mid^{-\beta}\cos\tau\omega d\omega$$

and let $x = \omega - \omega_0$ from which we obtain

$$R(\tau) = \int_{-\omega_0}^{\pi-\omega_0} b(x+\omega_0) \mid x \mid^{-\beta}\cos[\tau(x+\omega_0)]dx$$

Let $b_1(x) = b(x+\omega_0)$. Obviously $b_1(x)$ is slowly varying at $x=0$ from the right and of bounded variation in $(-\omega_0,-\varepsilon) \cup (\varepsilon,\pi-\omega_0)$. We can

write

$$R(\tau) = \int_{-\omega_0}^{\pi-\omega_0} |x|^{-\beta} b_1(x)(\cos(\tau x)\cos(\tau\omega_0) - \sin(\tau x)\sin(\tau\omega_0))dx$$

$$= \int_{-\omega_0}^{\pi-\omega_0} |x|^{-\beta} b_1(x)\cos(\tau x)\cos(\tau\omega_0)dx - \int_{-\omega_0}^{\pi-\omega_0} |x|^{-\beta} b_1(x)$$

$$\bullet \sin(\tau x)\sin(\tau\omega_0)dx$$

$$= S_1 - S_2 .$$

$$S_1 = \int_{-\omega_0}^{0} (-x)^{-\beta} b_1(x)\cos(\tau x)\cos(\tau\omega_0)dx + \int_0^{\pi-\omega_0} (x)^{-\beta} b_1(x)\cos(\tau x)\cos(\tau\omega_0)dx$$

$$= S_{11} + S_{12} .$$

Now, $S_{12} = \cos(\tau\omega_0)\int_0^{\pi-\omega_0} x^{-\beta} b_1(x)\cos(\tau x)dx$

$$= \cos(\tau\omega_0) \int_0^{\pi} x^{-\beta} b_1(x)\cos(\tau x)dx$$

where $b_1(x)$ has been extended to $(0,\pi)$ by letting

$$b_1(x) = 0 \quad \text{for } x \in [\pi-\omega_0,\pi).$$

Then, it follows that $b_1(x)$ is of bounded variation in any interval (ε,π) where $0 < \varepsilon < \pi$, and by Theorem 2.24 Zygmund,

$$S_{12} \simeq \cos(\tau\omega_0)\ b_1(\tfrac{1}{\tau})\ \sin(\tfrac{\pi\beta}{2})\tau^{\beta-1} .$$

Now for S_{11} we have

$$S_{11} = \int_{-\omega_0}^{0} (-x)^{-\beta} b_1(x)\cos(\tau x)\cos(\tau\omega_0)dx$$

$$= \cos(\tau\omega_0) \int_0^{\omega_0} \omega^{-\beta} b_1(-\omega)\cos(\tau\omega)d\omega .$$

Let $b_2(\omega) = b_1(-\omega)$, and it follows that $b_2(\omega)$ is slowly varying at 0 from the right and of bounded variation in any interval $(0, \omega_0-\varepsilon)$ for $0 < \varepsilon < \omega_0$. Extending $b_2(x)$ to $(0,\pi)$ by letting

$$b_2(x) = 0 \text{ for } x\varepsilon[\omega_0,\pi],$$

then

$$S_{11} = \cos(\tau\omega_0)\int_0^{\pi} \omega^{-\beta} b_2(\omega)\cos(\tau\omega)d\omega \quad .$$

Again by Zygmund, Theorem 2.24 and the same argument used for S_{12},

$$S_{11} \simeq \cos(\tau\omega_0)b_2(\tfrac{1}{\tau}) \sin(\tfrac{\pi\beta}{2})\tau^{\beta-1} \quad .$$

Hence

$$S_1 \simeq \cos(\tau\omega_0)\sin(\tfrac{\pi\beta}{2})\tau^{\beta-1} \left[b_1(\tfrac{1}{\tau}) + b_2(\tfrac{1}{\tau})\right] \quad .$$

Considering

$$S_2 = \int_{-\omega_0}^{\pi-\omega_0} |x|^{-\beta} b_1(x) \sin(\tau x)\sin(\tau\omega_0)dx \ ,$$

the same argument used for S_1 shows that

$$S_2 \simeq \sin(\tau\omega_0)\cos(\tfrac{\pi\beta}{2})\tau^{\beta-1}\left[b_1(\tfrac{1}{\tau}) + b_2(\tfrac{1}{\tau})\right].$$

Therefore

$$R(\tau) = S_2 - S_1$$

$$\simeq \tau^{\beta-1}\left[b_1(\tfrac{1}{\tau}) + b_2(\tfrac{1}{\tau})\right]\left[\cos(\tau\omega_0)\sin(\tfrac{\pi\beta}{2}) - \sin(\tau\omega_0)\cos(\tfrac{\pi\beta}{2})\right]$$

$$= \tau^{\beta-1}\left[b_1(\tfrac{1}{\tau}) + b_2(\tfrac{1}{\tau})\right] \sin(\tfrac{\pi\beta}{2} - \tau\omega_0)$$

i.e.

$$R(\tau) \simeq \tau^{\beta-1} \sin(\tfrac{\pi\beta}{2} - \tau\omega_0) \left[b_1(\tfrac{1}{\tau}) + b_2(\tfrac{1}{\tau})\right] \text{ when } \tau\to\infty.$$

which completed the proof of the lemma.

Returning to the proof of (c), we see that for a Gegenbauer process with $|u| < 1$, the spectrum $P(\omega)$ is given by

$$P(\omega) = \sigma_a^2\left[4(\cos\omega-u)^2\right]^{-\lambda} \quad .$$

Letting $\omega_0 = \cos^{-1}u$, then

$$P(\omega) = \sigma_a^2 \left[2 \sin^2(\frac{\omega-\omega_0}{2}) \sin^2(\frac{\omega+\omega_0}{2})\right]^{-\lambda}.$$

Write $P(\omega) = |\omega-\omega_0|^{-2\lambda} b(\omega)$

with $b(\omega) = \sigma_a^2\, 2^{-\lambda}[\sin^2(\frac{\omega+\omega_0}{2})]^{-\lambda}\left[\left[\frac{\sin(\frac{\omega-\omega_0}{2})}{\omega-\omega_0}\right]^2\right]^{-\lambda}$.

We demonstrate that $b(\omega)$ satisfies the conditions in the Lemma.

i) The fact that $b(\omega)$ is of bounded variation in $(0,\omega_0-\varepsilon)\cup(\omega_0+\varepsilon,\pi)$ can be easily shown.

ii) To show that $b(\omega)$ is slowly varying at ω_0 we consider the case $\omega > \omega_0$. Let

$$\ell(\omega) = (\omega-\omega_0)^{\delta} b(\omega)$$

$$= 4^{-\lambda}(\omega-\omega_0)^{2\lambda+\delta}[(\cos\omega - \cos\omega_0)^2]^{-\lambda}\,\sigma_a^2 \quad .$$

Then,

$$\frac{d\ell(\omega)}{d\omega} = \sigma_a^2\, 4^{-\lambda}(\omega-\omega_0)^{\delta+2\lambda-1}(\cos\omega_0 - \cos\omega)^{-2\lambda-1}$$

$$[(\delta+2\lambda)(\cos\omega_0 - \cos\omega) - 2\lambda(\omega-\omega_0)\sin\omega].$$

When $\omega > \omega_0$, $(\omega-\omega_0)^{\delta+2\lambda-1}$ and $(\cos\omega_0 - \cos\omega)^{-2\lambda-1}$ are positive. For $(\delta + 2\lambda)(\cos\omega_0-\cos\omega)-2\lambda(\omega-\omega_0)\sin\omega$, when $\omega \downarrow \omega_0$ both terms approach zero. However using L'Hospital rule it can be shown that

$$\lim_{\omega\downarrow\omega_0} \frac{2\lambda(\omega-\omega_0)\sin\omega}{(\delta+2\lambda)(\cos\omega_0 - \cos\omega)} = \frac{2\lambda}{\delta+2\lambda} < 1.$$

Hence when ω approaches ω_0 from right and is sufficiently close,

$$(\delta+2\lambda)(\cos\omega_0 - \cos\omega) - 2\lambda(\omega-\omega_0)\sin\omega > 0.$$

Thus $\frac{d\ell(\omega)}{d\omega} > 0$ in some right-hand neighborhood of ω_0 and $(\omega-\omega_0)^{\delta}b(w)$ is increasing when ω approaches ω_0 in some right-hand neighborhood of ω_0. Similarly $(\omega-\omega_0)^{-\delta}b(\omega)$ decreases in some right-hand neighborhood of ω_0. Using the same argument, it can be shown that $(\omega_0-\omega)^{\delta}b(\omega)$ decreases and $(\omega_0-\omega)^{-\delta}b(\omega)$ increases in some left-hand neighborhood of ω_0 when ω approaches ω_0. Therefore $b(\omega)$ is slowly varying at ω_0 and by the Lemma, $\rho(\tau)$ has the property that

$$\rho(\tau) \simeq \tau^{2\lambda-1}\sin(\pi\lambda - \tau\omega_0)\left[b_1(\tfrac{1}{\tau}) + b_2(\tfrac{1}{\tau})\right]$$

as $\tau \to \infty$. However, $b_1(1/\tau) + b_2(1/\tau)$ approaches a finite, nonzero constant as $\tau\to\infty$, and thus as $\tau\to\infty$,

$$\rho(\tau) \simeq \tau^{2\lambda-1}\sin(\pi\lambda-\tau\omega_0) \ .$$

4. The GARMA Process

In the same manner that the fractional process has been extended to FARMA processes, we now extend the Gegenbauer process by combining it with the ARMA process. This leads to the following definition.

Definition 5: If $\phi(B)$ and $\theta(B)$ are defined as in (3), then we define the Gegenbauer-ARMA (GARMA) process by

$$\phi(B)(1-2uB + B^2)^{\lambda}(X(t)-\mu) = \theta(B)a(t). \tag{17}$$

Theorem 4 summarizes properties of the GARMA process.

Theorem 4. Let $\{X(t)\}$ be a GARMA (p,u,λ,q) process $(\lambda \neq 0)$ and let all roots of $\phi(Z) = 0$ and $\theta(Z) = 0$ lie outside the unit circle. Then

a) $\{X(t)\}$ is stationary if $\lambda < 1/4$ when $u = \pm 1$ or $\lambda < \frac{1}{2}$ when $|u| < 1$;

b) $\{X(t)\}$ is invertible and if $\lambda > -1/4$ when $u = \pm 1$ or $\lambda > -\frac{1}{2}$ when $|u| < 1$;

c) if $0 < \lambda < 1/4$ when $u = \pm 1$ or $0 < \lambda < \frac{1}{2}$ when $|u| < 1$, then $\{X(t)\}$ is a long memory process.

d) (i) if $|u| < 1$, $\lim_{\omega\to\omega_0} (\omega-\omega_0)^{2\lambda}P(\omega)$ exists and is finite.

(ii) if $|u| = 1$, $\lim_{\omega\to\omega_0} (\omega-\omega_0)^{4\lambda}P(\omega)$ exists and is finite.

e) as $\tau \to \infty$,

(i) $\rho(\tau) \simeq \tau^{4\lambda-1}$ when $u=1$ and $0<\lambda<1/4$

(ii) $\rho(\tau) \simeq (-1)^{\tau}\tau^{4\lambda-1}$ when $u=-1$ and $0<\lambda<1/4$

(iii) $\rho(\tau) \simeq \tau^{2\lambda-1}\sin(\pi\lambda-\tau\omega_0)$ when $|u| < 1$, $0<\lambda<1/2$ and ω_0 is the G-frequency.

Proof: The proofs of (a) and (b) are obvious (cf. Hosking (1981), Theorem 2). For part (c) note that

$$P(\omega) = \sigma_a^2 \frac{|\theta(e^{i\omega})|^2}{|\phi(e^{i\omega})|^2} \left| 1-2ue^{i\omega} + e^{2i\omega} \right|^{-2\lambda}$$

$$= \sigma_a^2 \frac{|\theta(e^{i\omega})|^2}{|\phi(e^{i\omega})|^2} \left[2(\cos\omega-\cos\omega_0)\right]^{-2\lambda}$$

where $\omega_0 = \cos^{-1}u$, is the G-frequency.

Part d(i) can be seen by writing $P(\omega)$ as

$$P(\omega) = \sigma_a^2 \frac{|\theta(e^{i\omega})|^2}{|\phi(e^{i\omega})|^2} \left[4\sin(\frac{\omega-\omega_0}{2})\sin(\frac{\omega+\omega_0}{2})\right]^{-2\lambda}$$

while d(ii) follows from Hosking (1981). The proof of e(i) was given by Hosking (1981) and e(ii) follows along the same lines. Result e(iii) is shown using the Lemma in the proof of Theorem 3c. That is,

$$P(\omega) = \sigma_a^2 \frac{|\theta(e^{i\omega})|^2}{|\theta(e^{i\omega})|^2} [4(\cos\omega - \cos\omega_0)^2]^{-\lambda}$$

can be written in the form $P(\omega) = |\omega - \omega_0|^{-2\lambda} b(\omega)$ where $b(\omega)$ is of bounded variation in $(0,\omega_0-\varepsilon) \cup (\omega_0+\varepsilon,\pi)$ and is slowly varying at ω_0.

5. Simulated Realizations from GARMA Models

(a) Generating Realizations from GARMA Models

Hosking (1984) suggests an algorithm for simulating realizations from a FARMA model which utilizes the autocovariance function. Since there is not a closed form expression for the covariance of a Gegenbauer process, it was decided to generate the realizations directly from Equation (7). Of course in practice this infinite series will require truncation, and our realizations X(t) were generated using

$$X(t) = \mu + \sum_{k=0}^{M} C_k^{(\lambda)}(u)a(t-k) \tag{18}$$

with M = 290,000. Using this truncation, the variance of the process appeared to be correct to at least two decimal places for the models considered here. As can be seen by inspecting the figures which follow, the sample correlations verify that the simulated series posses the proper correlation structure. Although this procedure is

time consuming, one advantage to computing the realizations in this manner is that each realization can be generated from the same random number seed, and thus differences in the realizations are due entirely to the differing parameters and not the noise.

Realizations from the GARMA model were obtained using a procedure described by Hosking (1984) for the FARMA model. In particular, in order to generate a realization from the GARMA model in (17), we, first rewrite this model as

$$\begin{aligned}\phi(B)(X(t)-\mu) &= (1-2uB + B^2)^{-\lambda}\theta(B)a(t) \\ &= \theta(B)Z(t)\end{aligned}$$

where $Z(t) = (1-2uB + B^2)^{-\lambda}a(t)$, i.e., Z_t is a Gegenbauer process given by $(1-2uB + B^2)^{\lambda}Z(t) = a(t)$ and a realization from this process can be simulated using the technique described in the preceding paragraph. A realization from the GARMA process X(t) can then be obtained using

$$X(t)-\mu = \sum_{j=1}^{p} \phi_j(X(t-j)-\mu) + Z(t) - \sum_{j=1}^{q} \theta_j Z(t-j) \tag{19}$$

From (19) it is obvious that the starting values Z(k), k=0,-1,...,1-q will be required along with X(k), k=0,-1,...,1-p. While starting values Z(k) are easily obtained from (18), the starting values X(k) are not as easily obtained. Hosking (1984) recommends a procedure for initializing the X(t) process with p starting values of zero, generating n+L values of X(t) using (19) and retaining the last n of these values of X(t) as the realization X(t), t=1,...,n. Hosking provides guidelines for the selection of L. In the realizations shown here we take L=150.

(b) Simulation Results

The simulated realizations shown in this section are based on $\mu=0$. Also, in the remainder of this paper we find it more convenient to use normalized frequency, i.e. $f = \omega/(2\pi)$. Thus, we use the notation, f_0, to denote the normalized G-frequency, i.e. $f_0 = \omega_0/(2\pi)$. Figure 2a shows a realization of length 500 from the Gegenbauer process with $u = .8$ and $\lambda = .45$, and $a(t) \sim N(0,1)$, i.e.

$$(1-1.6B + B^2)^{0.45}X(t) = a(t) \ . \tag{20}$$

The operator in the parenthesis has a G-frequency of $f_0 = .10$ associated with it. The periodicity induced by this operator is apparent. Figure 2b shows only the first 100 of these same sample values. On this larger scale the periodicity just referred to is more apparent.

Figure 2c and 2d show the resulting true and sample autocorrelations. The agreement is quite good. An ARMA process was fit to this data via the S-array method (see Gray, Kelley and McIntire (1978)) and the model obtained was

$$X(t) - 1.555X(t-1) + .943X(t-2) = a(t) + a(t-1) \ , \tag{21}$$

which also has a system frequency of $f_0 = .10$ associated with it. It is interesting to note that the periodic nature of the data is captured in (21) but that the autocorrelation associated with (21) would decay much too fast even though it is very close to the nonstationary region.

Figure 3a shows a realization of length 500 from the Gegenbauer process with $u = -.8$ and $\lambda = .45$. This is much higher frequency data than that of Figure 2, having a G-frequency of $f_0 = .40$ associated with it. The data and the true autocorrelation, shown in Figure 3b

clearly reflect this difference. The sample autocorrelation for this data is given in Figure 3c.

The realizations shown thus far have shown the impact of changing u in the Gegenbauer process. Figure 4a shows the first 100 values of a realization of length 500 from a Gegenbauer process, again with u = .8 but this time with λ = .2. Clearly the G-frequency is not as persistent in the data as when λ = .45. Fitting an ARMA process to this data leads to the MA(2) model

$$X(t) = -.342a(t-1) - .118a(t-2) + a(t)$$

which completely misses the presences of a periodic component. Thus unless the process is near the nonstationary region it appears that fitting an ARMA model to the data would lead not only to a model for which the memory is too short, but to a model which total misses the most salient features of the data. Figure 4b gives the true autocorrelations and it can be seen that although these autocorrelations are small, they do damp slowly. Figure 4c gives the sample autocorrelation where the sinusoidal behavior is not as evident but is still discernible.

In Figure 5a we display a realization of length n=500 from the GARMA process

$$(1-.9B)(1-2uB+B^2)^{\lambda}X(t) = a(t) \qquad (22)$$

where u = .8 and λ = .45. Thus, the Gegenbauer component of this GARMA model is the same as that in the Gegenbauer process in (20) which is displayed in Figure 2. From Figure 5 we can see that the effect of the autoregressive factor 1-.9B is to induce a certain amount of wandering, nonperiodic behavior to the realization. In Figure 5b and 5c we show the true and sample autocorrelations from

this model. There it can be seen that for smaller lags, the damped exponential contribution associated with (1-.9B) is evident. At larger lags the sinusoidal nature of the autocorrelations is predominant, and although the amplitudes are smaller than those in Figure 2 they still tend to damp very slowly.

In Figure 6a we show a realization from the GARMA process

$$(1-.9B)(1+.8B)(1-2uB+B^2)^{\lambda}X(t) = a(t) \ . \qquad (23)$$

where u = .8 and λ = .3 while in Figures 6b and 6c we show the true and sample autocorrelations. While the purpose for introducing the FARMA and GARMA models was to model long memory behavior, it can be seen that the GARMA model of (23) shows no strong indication that the autocorrelation damps slowly. It seems possible, therefore, that the GARMA model might also prove to be useful for modeling time series in which long memory is not apparent.

In Figure 7a we display a realization from the GARMA process $(1+1.3B+.8B^2)(1-2(.8)B+B^2)^{.45}X(t) = a(t)$ while in Figures 7b and 7c we show the true and sample autocorrelation respectively. These autocorrelations display a very interesting pattern which deserves discussion. For low lags, i.e., $\tau \leq 25$, the autocorrelation clearly shows a high frequency behavior and not so clearly, a low frequency behavior. However, for higher lags, i.e., $\tau > 25$ there is a definite low frequency behavior associated with a frequency near .1 and little or no high frequency pattern. Thus, for this model, the autocorrelation function is dominated by the ARMA component, i.e. $(1+1.3B + .8B^2)$ for lower lags, but due to the slower decay associated with the Gegenbauer component, the factor $(1-1.6B+B^2)^{.45}$ dominates for higher lags. This asymptotic behavior of $\rho(\tau)$ is

consistent with Theorem 4 part e(iii).

6. Parameter Estimation and Model Identification

In order to estimate the parameters of the GARMA (p,u,λ,q) model in (17), we will use maximum likelihood (ML) methods. In this section we assume that p and q are known and that the white noise is normal. The problem of identifying p and q will also be discussed.

ML Estimation

The exact ML estimates can be found by the direct maximization of the likelihood function on the basis of the p+q+4 parameters $\phi_1,\ldots,\phi_p$, $\theta_1,\ldots,\theta_q$, μ, σ_a^2, u and λ. However, this is a very tedious procedure even in the FARMA case (see Hosking 1984), and in practice we use procedures for obtaining approximate ML estimates.

When obtaining approximate ML estimators, we first estimate μ by $\bar{X}$ and then follow the procedure used by Hosking (1984) for splitting the model into its Gegenbauer and ARMA components. Let $\beta = (\phi_1,\ldots,\phi_p, \theta_1,\ldots,\theta_q, \sigma_a^2)'$ and $\alpha = (\beta; u, \lambda)'$. Given u and λ, we transform to obtain

$$W(t) = (1-2uB + B^2)^{\lambda}(X(t) - \bar{X})$$

$$= \sum_{j=0}^{\infty} \pi_j (X(t-j) - \bar{X}). \tag{24}$$

The resulting process, W_t, is ARMA (p,q), i.e.

$$\phi(B)W(t) = \theta(B)a(t) \tag{25}$$

where $\phi(B)$ and $\theta(B)$ are as in (17). Since the Jacobian of the transformation in (24) is approximately one, it follows that

$$L(x,\alpha) \simeq L(w,\beta)$$

where L denotes the appropriate likelihood function. Since $L(w,\beta)$ is the likelihood of an ARMA(p,q), ML estimates of the parameters β can be found using ARMA-based maximum likelihood methods. In our implementation, we used IMSL subroutine FTML to obtain conditional ML estimates of β. The procedure for obtaining approximate ML estimates is to examine a grid of values for u and λ, transform to W(t) for each (u, λ) pair and maximize the likelihood function $L(w,\beta)$ for the transformed data. The approximate ML estimates of u and λ are the pair ($\hat{u}$, $\hat{\lambda}$) in the grid associated with the largest of the maximized likelihoods, and the approximate ML estimates of the parameters β are those which produced the largest maximized likelihood.

In order for the transformation in (24) to be used in practice, Hosking (1984) recommends truncating the series in (24) at M where M is chosen to be sufficiently large. He also suggests the use of backcasting to estimate X(-1),...,X(-M) based on the given data. In our implementation, we backcast by fitting an AR(12) model to the X_t series.

Model Identification

The maximum likelihood estimation involves known p and q, but of course in practice, p and q will not be known. Hosking (1984) used Akaike's (1974) AIC for identifying the orders p and q of a FARMA model, and we have considered an adaptation of this method to the GARMA model. AIC for the GARMA model in (17) is

$$AIC = -2\log L_{max} + 2(p+q+\delta) \tag{26}$$

where L_{max} is the maximized likelihood of the fitted model and $\delta = 2$ if a GARMA model is fit to the data, while $\delta = 0$ if the model is constrained to be ARMA (i.e. $\lambda = 0$). The implementation of the AIC model in practice would involve selecting several candidate models (possibly including cases in which $\lambda = 0$ and in which $\lambda \neq 0$), calculating the AIC criterion in (26) and selecting the model for which the AIC criterion is minimized.

7. Examples

In this section we consider the procedures discussed in Section 6 through three examples, two of which involve simulated realizations from GARMA models. The third example to be considered is the classical sunspot data.

Example 1.

In Figure 5 a realization of length 500 and the autocorrelations from the GARMA model

$$(1-\phi_1 B)(1-2uB + B^2)^{\lambda}(X(t)-\mu) = a(t) \tag{27}$$

where $\phi_1 = .9$, $u = .8$, $\lambda = .45$ and $\mu = 0$, were displayed. For the data of Figure 5, p and q are selected and the maximum likelihood estimates of u, λ, the ϕ_i and the θ_i were computed by the methods described in Section 6. Table 1 shows the AIC values for GARMA models with $0 \leq p \leq 3$, $0 \leq q \leq 2$ and for strictly AR(p) models, $1 \leq p \leq 3$. By that table we see that the AIC choice of models yields GARMA (1,0). The corresponding maximum likelihood estimates for the remaining parameters are $\hat{u} = .8$, $\hat{\lambda} = .48$ and $\hat{\phi}_1 = .89$. The estimated model is therefore

$$(1-.89B)(1-1.6B+B^2)^{.48}(X(t) - \bar{X}) = a(t), \qquad (28)$$

which is very close to the true model. Obtaining the result of Equation (28) is very computationally extensive. For this reason, we will now make some observations which will often lead to a substantial reduction in computation time with very little degradation in the resulting estimated model. In this case inspection of the sample autocorrelations in Figure 5(c) showed a clear persistence in the data in the neighborhood of f = .1. Since f = .1 corresponds to u = .8, the values of u considered could be restricted to $.7 \leq u \leq .9$, substantially reducing computer time. However, even with this reduction, the computation time would still be extensive. When there is a clear persistence in the sample autocorrelations, the method of overfitting an AR(p) process discussed by Gray and Woodward (1986) can be used to estimate u. That is, one fits a sequence of AR(p) processes for several large values of p and tables the factors by order of the proximity of their associate roots to the unit circle. One then considers only those factors with roots very near the unit circle as candidates for the "Gegenbauer factor" in the model. For the data shown in Figure 5, the corresponding factor table is given in Table 2 for an AR(20) fit. The factor associated with the frequency f=.10 is clearly the top contender for the Gegenbauer factor. The frequency f=.02 is also a possibility. Therefore one could limit the MLE range of consideration to the two values u = .8, u = .99. Also a quick glance at the sample autocorrelations in Figure 5(c) suggest that λ is not small, so it probably suffices to limit $.3 < \lambda < .5$. Taking $\lambda = .3$ and u = .8 as trial values and using the GPAC and S-array method to estimate p and q on the tranformed data, W(t), leads

immediately to the estimate $p = 1$ and $q = 0$. With this examination one could probably feel comfortable in restricting the parameter space to $\{u=.8,\ \lambda \geq .3,\ p = 1,\ q = 0\} \cup \{u=.99,\ \lambda \geq .3,\ p \leq 3,\ q \leq 2\}$. This leads to the same model as determined in (28). In short, a little prior analysis by the analyst may significantly reduce the compulation time with little appreciable degradation in the results. The sample autocorrelations in Figure 5d could be used to give an initial estimate of λ using the results given earlier concerning the form of the autocorrelations of a Gegenbauer process. For a Gegenbauer process, $\rho(k) \simeq k^{2\lambda-1}\sin(\pi\lambda-2\pi k f_0)$, so it follows that the distance from a peak down to the next trough of sample autocorrelations should fairly closely estimate $2Ck^{2\lambda-1}$ where k is the location of the peak and C is a finite, nonzero constant. Thus, if the "peak to trough" distance is found for two values of k, say k_1 and k_2, then if h_i is the "peak to trough" distance associated with k_i, we have

$$\frac{2Ck_1^{2\lambda-1}}{2Ck_2^{2\lambda-1}} \approx \frac{h_1}{h_2}$$

so that

$$\lambda \approx \left[\frac{\ln(h_1/h_2)}{\ln(k_1/k_2)} + 1 \right] /2.$$

Using this approximation on the sample autocorrelations in Figure 5c based on $k_1 = 49$ and $k_2 = 88$ we obtain $\hat{\lambda} = .41$. Other techniques for obtaining preliminary estimates of λ are possible. Basically, this estimation is based on the use of the sample autocorrelations to measure how fast the autocorrelations are damping.

In some cases this preliminary estimation of λ is not possible. We have seen that the GPAC identification of p and q using transformation to W(t) based upon preliminary estimates of u and λ, is quite insensitive to $\hat{\lambda}$ as long as u is estimated reasonbly well.

In the remaining examples such methods as described here were used to limit the number of models under consideration and the maximum likelihood estimates were obtained only for this reduced collection of models.

Example 2. In Figure 6 we showed a realization and the autocorrelations for the GARMA model

$$(1-.9B)(1+.8B)(1-2uB+B^2)^{\lambda}X(t) = a(t)$$

i.e.

$$(1-\phi_1 B-\phi_2 B^2)(1-2uB+B^2)^{\lambda}X(t) = a(t)$$

where u=.8 and λ=.3, ϕ_1=.1 and ϕ_2=.72. There it was seen that the sample autocorrelations were not clearly slowly dampling so that visually, there may not have been an indication that the process in Figure 6a was from a GARMA process. The factor table for an AR(20) overfit is given in Table 3. There it can be seen that two frequencies appear to be strong, one around f=.1 and the other near f=0. These frequencies are associated with values of u near .8 and 1 respectively and thus we have restricted the range of u values in the ML search accordingly. Considering GARMA models for $0 \leq p \leq 3$ and $0 \leq q \leq 3$ using the grid of (u,λ) values with $0.7 \leq u \leq 0.99$, $0.20 \leq \lambda \leq 0.45$ with .01 increment and strictly AR(p) models with $1 \leq p \leq 4$, AIC picked p=2 and q=0. The ML estimates were $\hat{u}$ = .80, $\hat{\lambda}$ = .34, $\hat{\phi}_1$ = .06 and $\hat{\phi}_2$ = .74. Transforming X(t) to obtain W(t) resulted

in ARMA(2,0) identification by GPAC as long as the $\hat{u}$ used in the transformation was close to .8. It should be noted that estimation of λ from the sample autocorrelations does not seem plausible in this case.

Example 3. Sunspot Data

In Figure 8 we show the 176 yearly sunspot averages from 1749 to 1924 along with the sample autocorrelations. The data shows the pseudo-periodic behavior which has interested scientists for centuries, and the autocorrelations have a slowly dampling sinusoidal appearance similar to the autocorrelations to Gegenbauer and GARMA processes shown earlier. In Table 4 we display the factor table associated with an AR(15) overfit from which we estimate u to be approximately $\cos[2\pi(.09)] = .84$. Preliminary estimation of λ as in Example 1 suggests that λ is approximately .3. Transforming the sunspot data using these values of u and λ, the GPAC array for the resulting W(t) series indicates an ARMA(8,0), ARMA(8,1) or possibly an ARMA(1,0). In the literature, several ARMA models have been proposed for the sunspot data. Box and Jenkins (1975) suggest an ARMA(2,0), Ozaki (1977) found an ARMA(8,0) to be the model selected by AIC and Woodward and Gray (1978) recommended an ARMA(8,1) on the basis of the S-array. We thus used AIC to compare the six models ARMA(2,0), ARMA(8,0), ARMA(8,1), GARMA(1,0), GARMA(8,0) and GARMA(8,1). AIC values for these models are shown in Table 5. On the basis of this comparison AIC selects the ARMA(8,0) with a GARMA(8,0) and GARMA (1,0) being a very close second and third choice. Thus the GARMA (1,0) is an attractive choice due to its parsimony and low AIC value. In Table

5 for each GARMA model, we show the ML estimates of u and λ. We have also tabled the dominant frequency for each model considered. For the GARMA models this is the Gegenbauer frequency, f_0, while for strictly ARMA models we table the frequency associated with the roots closest to the unit circle.

We also used the models mentioned in the preceding paragraph to produce forecasts. The procedure used for forecasting using the GARMA model was to transform the ARMA process $W(t) = (1-2uB+B^2)^{\lambda}X(t)$, find forecasts for the W(t) process using ARMA techniques and convert these to forecasts for X(t) using the fact that $X(t) = (1-2uB+B^2)^{-\lambda}W(t)$ and truncating the operator to a finite number of terms. In Table 5 we display mean square forecast errors for each model associated with forecasts from three blindly chosen forecast origins, t_0 = 156, 146 and 141. From each origin we forecast to the end of the realization, i.e. from t_0 = 156 we forecast 20 steps ahead, from t_0 = 146 we forecast 30 values while 35 forecast were obtained from t_0 = 141. It is clear from the table that from these forecast origins, the GARMA forecasts are superior.

8. Concluding Remarks

The FARMA process has been extended to the GARMA processes, and the latter has also been shown to be long memory. The significance of this extension is the inclusion of periodic or quasi periodic data in the long memory model. A more general GARMA model is currently being investigated which involves $m \geq 1$ Gegenbauer factors, i.e.

$$\phi(B) \prod_{i=1}^{m} (1-2u_iB + B^2)^{\lambda_i}X(t) = \theta(B)a(t).$$

An additional area of potential interest concerns the models on the dotted boundary of the stationary, long memory region shown in Figure 1. These are nonstationary processes which border the stationary region much as the first order process $(1-B)X(t) = a(t)$ borders the stationary region for AR(1) processes. It is interesting to note that this nonstationary AR(1) process is represented by the upper right-hand corner of the stationary, long memory region shown in Figure 1. It remains to be seen whether other nonstationary models on the boundary of the rectangle in Figure 1 will provide useful nonstationary models.

REFERENCES

Gradshteyn, J.S. and Ryzhik, I.W. (1965). Table of Integrals, Series and Products. New York: Academic Press.

Geweke, J. and Porter-Hudak, S. (1983). The estimators and application of long memory time series models. Journal of Time Series Analysis 4, 221-38.

Granger, C.W.J. and Joyeux, R. (1980). An introduction to long memory time series models and fractional differencing. Journal of Time Series Analysis 1, 15-29.

Gray, H. L., Kelley, G. D. and McIntire, D. D. (1978), "A New Approach to ARMA Modeling", Communications in Statistics B7, 1-77.

Gray, H. L. and Woodward, W. A. (1986), A New Spectral Estimator, Journal of American Statistical Association 81, 1100-1108.

Hosking, J.R.M. (1981). Fractional differencing, Biometrika 68, 1, 165-176.

Hosking, J.R.M. (1984). Modeling persistence in Hydrological time series using fractional differencing, Water Resource Research 20, 12, 1898-1908.

McLeod, Angus, I. and Hipel, K.W. (1978). Preservations of the rescaled adjusted range, 1. A reassessment of the Hurst phenomenon. Water Resource Research, 14, 491-508.

Magnus, W., Oberhettinger, F. and Soni, R. P. (1966). Formulas and Theorems for the special functions of Mathematical Physics, Berlin: Springer-Verlag.

Ozaki, T. (1977). "On the Older Determination of ARIMA Models." Applied Statistics 26, 290-301.

Rainville, E. D. (1960). Special Functions. New York: The Macmillan Company.

Waldmeier, M. (1961). The Sunspot Activity in the Years 1610-1960. Zurich: Zurich Schulthess and Co.

Woodward, W. A. and Gray, H. L. (1978). ARMA Models for Wolfers' Sunspot Data. Communications in Statistics B7, 97-115.

Woodward, W. A. and Gray, H. L. (1981). On the Relationship Between the S-Array and the Box-Jenkins Method of ARMA Model Identification, Journal of the American Statistical Association 76, 579-587.

Zygmund, A. (1959). Trigonometric Series, London: Cambridge University Press.

TABLE 1
AIC Values for Models Fitted to the Realization of Example 1

GARMA Models

q \ p	0	1	2	3
0	-	-49.60	-47.10	-44.38
1	339.69	-47.64	-45.06	-42.36
2	153.03	-46.08	-43.17	-45.63

AR (p) Models

p = 1	p = 2	p = 3
808.69	152.95	77.63

Table 2
Factor Table for GARMA Realization of Example 1

Absolute Reciprocal of Root (V)	Frequency (f)	Factors
.9894	.10	$1 - 1.579B + .979B^2$
.9534	.01	$1 - 1.896B + .909B^2$
.9107	.07	$1 - 1.671B + .829B^2$
.8936	.15	$1 - 1.007B + .798B^2$
.8846	.37	$1 + 1.212B + .783B^2$
.8837	.30	$1 + .569B + .781B^2$
.8681	.21	$1 - .424B + .754B^2$
.8119	.47	$1 + 1.605B + .659B^2$
.7929	.26	$1 + .084B + .629B^2$
.7823	.43	$1 + 1.430B + .612B^2$

Table 3
Factor Table for GARMA Realization of Example 2

Absolute Reciprocal of Root (V)	Frequency (f)	Factors
.9405	.02	$1 - 1.870B + .884B^2$
.9381	.10	$1 - 1.490B + .880B^2$
.8819	.38	$1 + 1.255B + .778B^2$
.8774	.16	$1 - .921B + .770B^2$
.8751	.07	$1 - 1.588B + .766B^2$
.8742	.22	$1 - .331B + .764B^2$
.8652	.49	$1 + 1.725B + .749B^2$
.8589	.45	$1 + 1.616B + .738B^2$
.8415	.29	$1 + .406B + .708B^2$
.7674	.31	$1 + .565B + .589B^2$

Table 4
Factor Table for Sunspot Data based on p=15

Absolute Reciprocal of Root (V)	Frequency (f)	Factors
.9538	.09	1 - 1.593B + .910B
.9278	.00	1 - .928B
.8741	.35	1 + 1.037B + .764B
.8371	.26	1 + .109B + .701B
.8313	.19	1 - .575B + .691B
.7965	.45	1 + 1.500B + .634B
.7787	.50	1 + .779B
.7208	.13	1 - .996B + .520B
.5500	.00	1 - .550B

TABLE 5
AIC Values, Parameter Estimates and Forecast Errors for Models Fitted to the Sunspot Data

Model	Model Parameters	AIC Value	Mean Square Forecast Errors from Origin t_0		
			$t_0 = 156$	$t_0 = 146$	$t_0 = 141$
ARMA (8,0)	$(1-1.25B+.51B^2+.13B^3-.18B^4+.16B^5-.08B^6+.13B^7-.21B^8)(X_t-44.78)=a_t$	959.93	505.64	883.79	691.04
GARMA (8,0)	$(1-.69B+.13B^2+.14B^3-.14B^4+.05B^5-.07B^6+.07B^7-.20B^8)(1-1.7B+B^2)^{.32}(X_t-44.78) = a_t$	960.72	278.18	451.49	361.37
GARMA (1,0)	$(1-.49B)(1-1.7B+B^2)^{.42}(X_t-44.78) = a_t$	960.75	328.89	437.65	355.06
ARMA (8,1)	$(1-1.49B+.80B^2+.03B^3-.22B^4+.21B^5-.12B^6+.12B^7-.18B^8)(X_t-44.78) = (1-.26B)a_t$	961.13	478.38	859.50	668.51
GARMA (8,1)	$(1-1.07B+.39B^2+.09B^3-.19B^4+.10B^5-.09B^6+.08B^7-.17B^8)(1-1.7B+B^2)^{.33}(X_t-44.78) = (1-.41B)a_t$	961.20	239.16	465.48	349.83
ARMA (2,0)	$(1-1.34B+.65B^2)(X_t-44.78) = a_t$	967.08	730.29	730.37	708.31

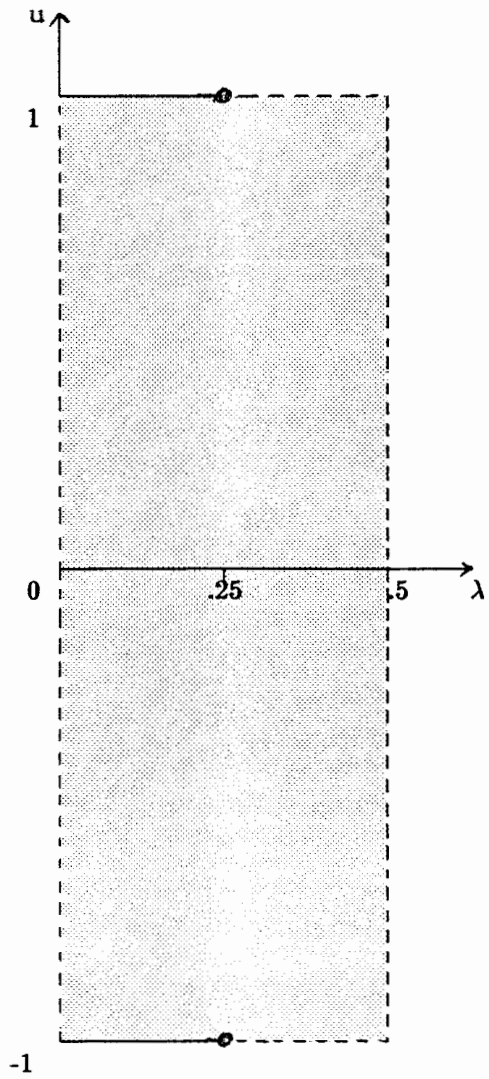

Figure 1 Stationary Long Memory Region of the Gegenbauer Process in (14)

Figure 2 - Realization and Autocorrelations for the Gegenbauer Process $(1-2(.8)B+B^2)^{.45}\ X(t) = a(t)$

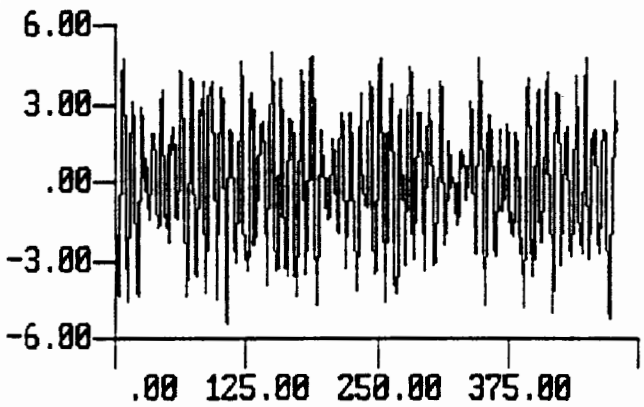

(a) Realization

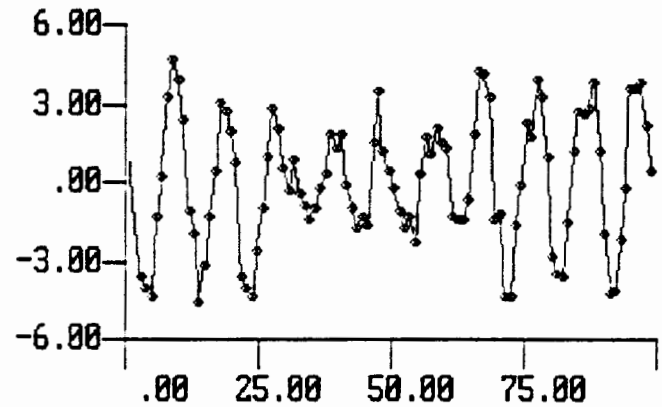

(a) Realization - First 100 Values

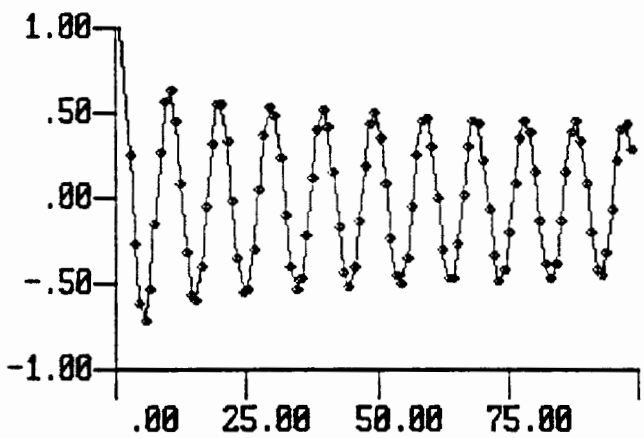

(c) True Autocorrelations

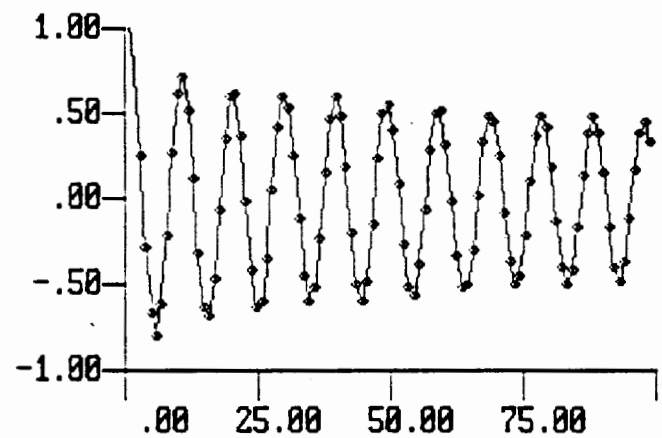

(d) Sample Autocorrelations

Figure 3 - Realization and Autocorrelations from the Gegenbauer Process $(1-2(-.8)B+B^2)^{.45}\ X(t) = a(t)$

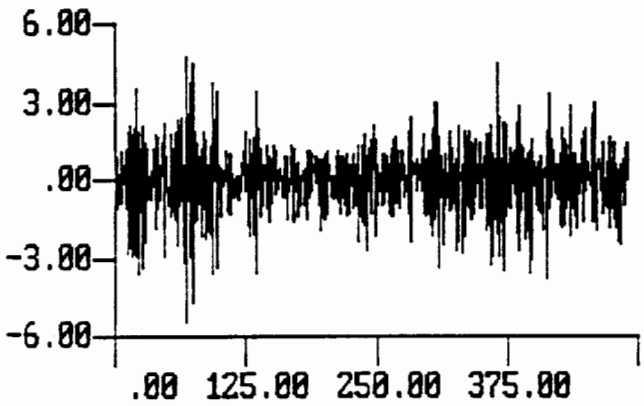

(a) Realization

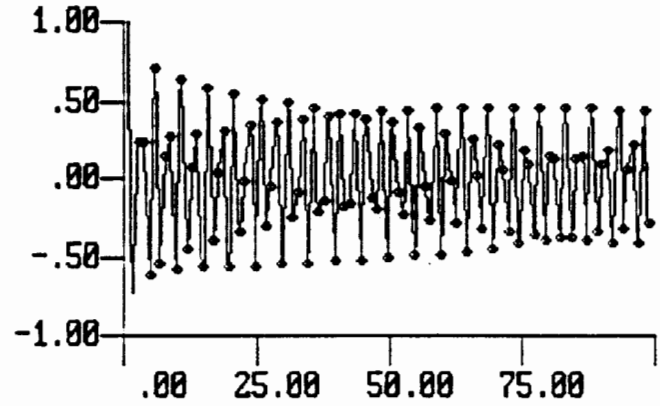

(b) True Autocorrelations

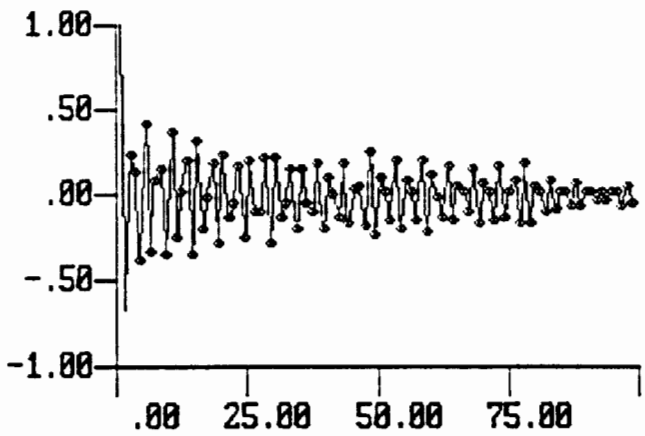

(c) Sample Autocorrelations

Figure 4 - Realization and Autocorrelations from the Gegenbauer Process $(1-2(.8)B+B^2)^{.2}\ X(t) = a(t)$

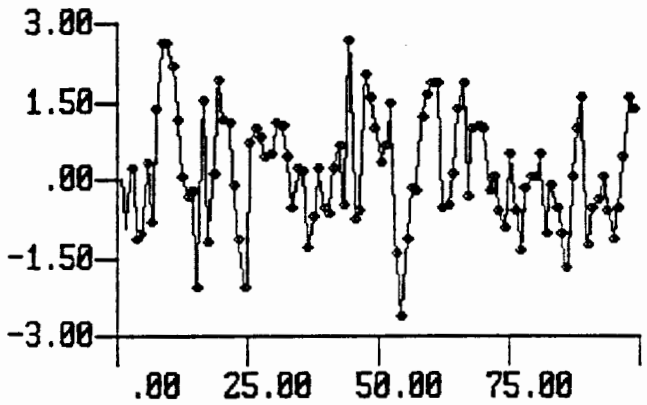

(a) Realization - First 100 Values

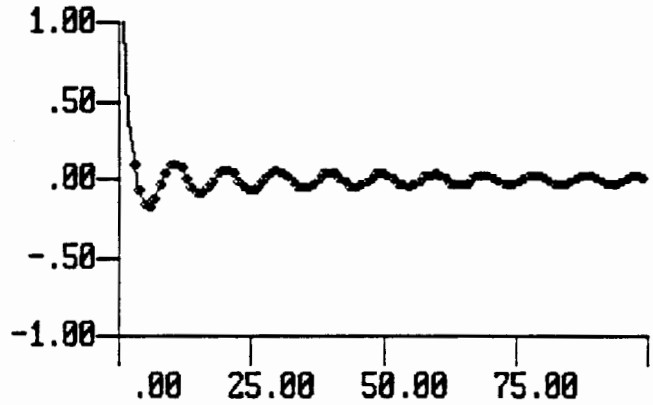

(b) True Autocorrelations

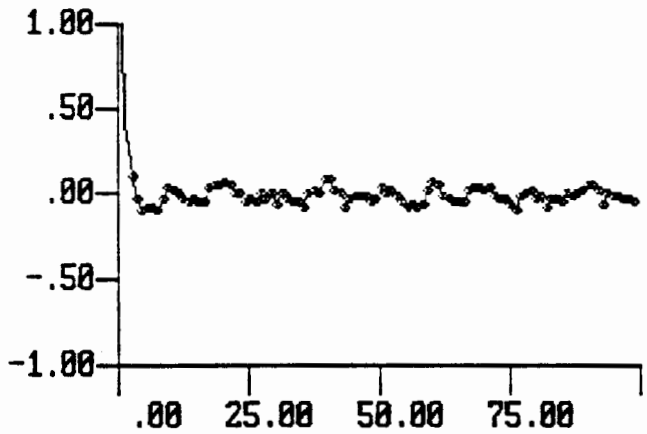

(c) Sample Autocorrelations

Figure 5 - Realization and Autocorrelations from the GARMA Model

$$(1 - .9B)(1 - 2(.8)B+B^2)^{.45} X(t) = a(t)$$

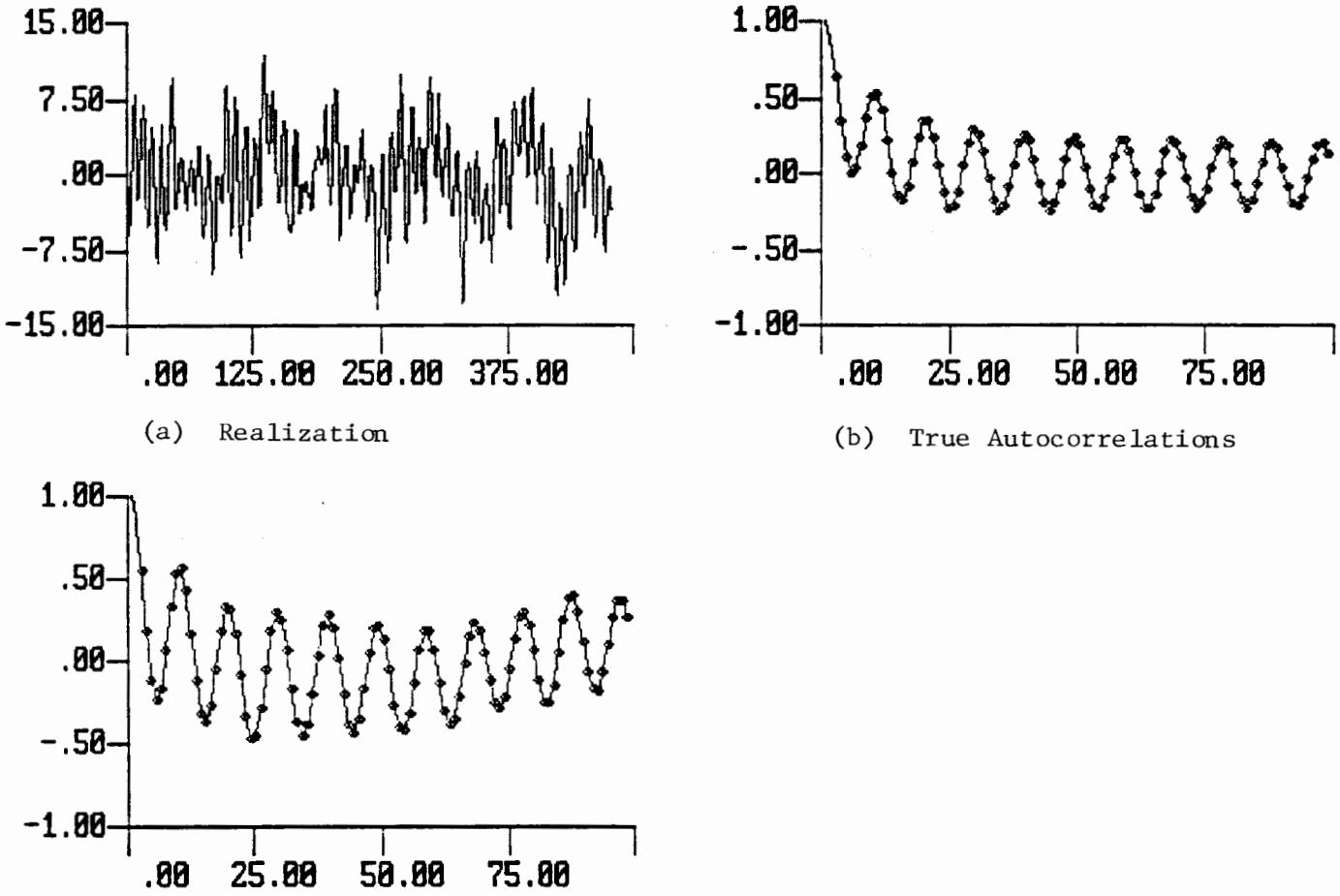

(a) Realization

(b) True Autocorrelations

(c) Sample Autocorrelations

Figure 6 - Realization and Autocorrelations from the GARMA Model

$$(1 - .9B)(1 + .8B)(1 - 2(.8)B+B^2)^{.3}\ X(t) = a(t)$$

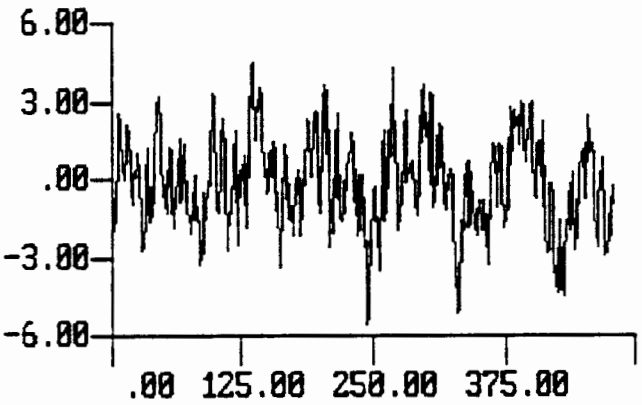

(a) Realization

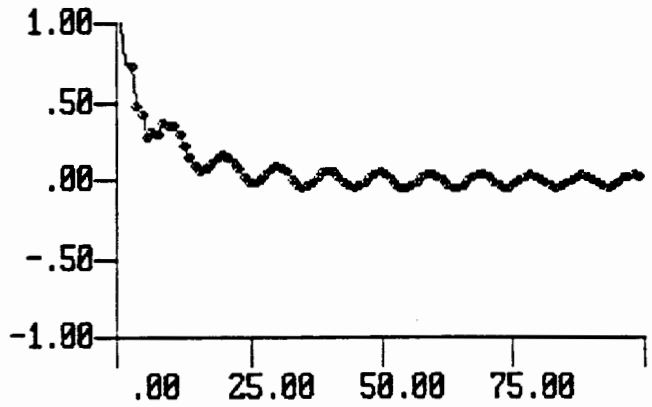

(b) True Autocorrelations

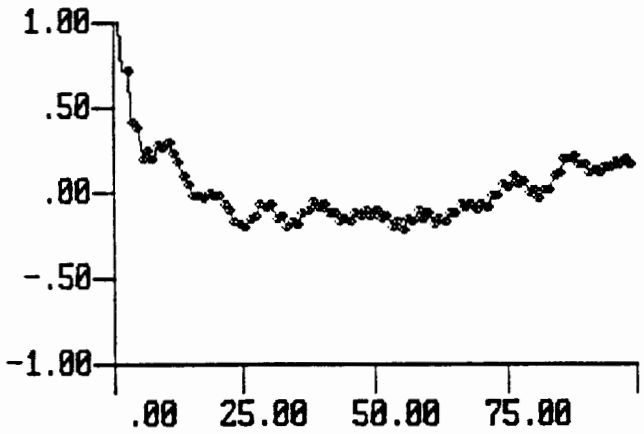

(c) Sample Autocorrelations

Figure 7 - Realization and Autocorrelations from the GARMA Model

$$(1 + 1.3B^2)\ (1 - 2(.8)B+B^2)^{.45}\ X(t) = a(t)$$

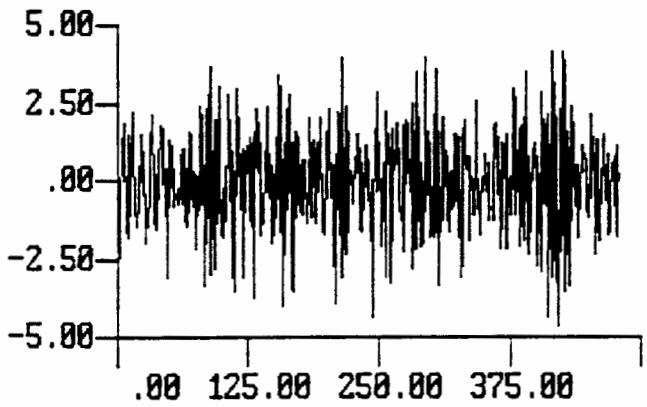

(a) Realization

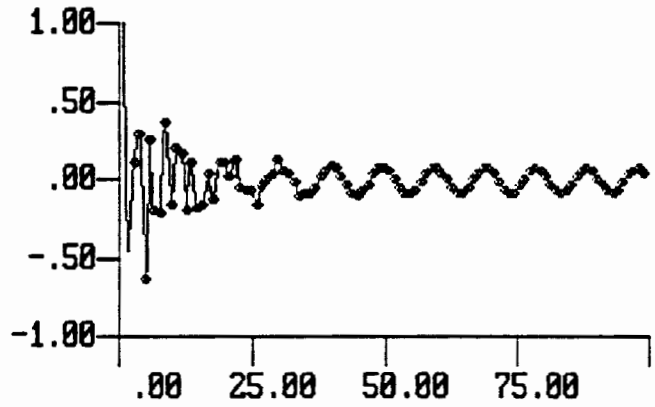

(b) True Autocorrelations

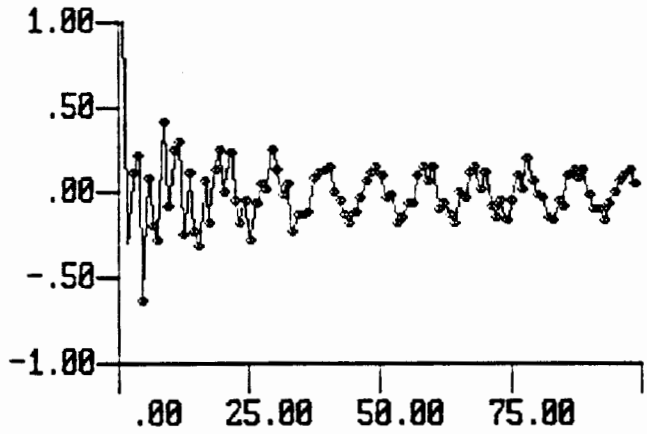

(c) Sample Autocorrelations

FIGURE 8

Yearly Sunspot Numbers from 1749 to 1924
and Sample Autocorrelations

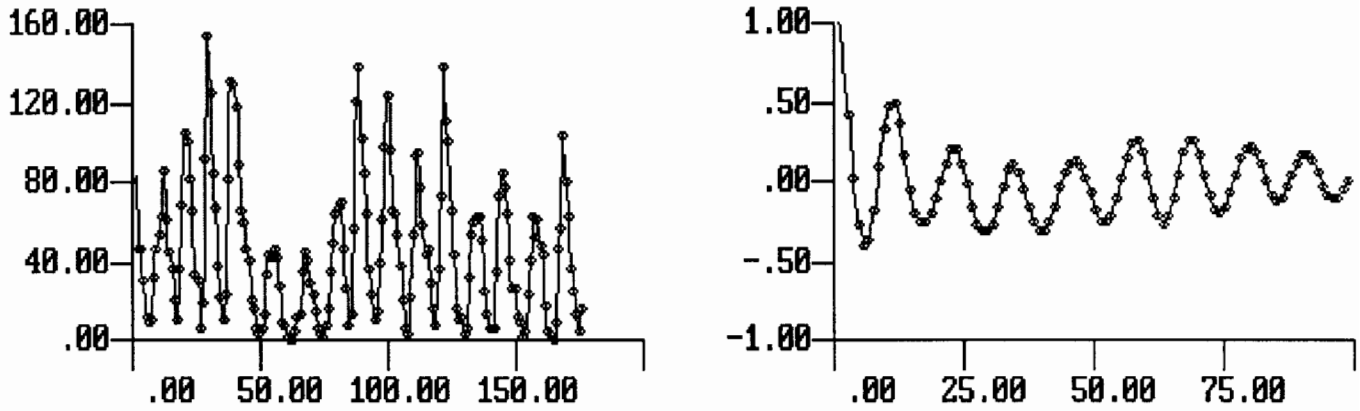

(a) Sunspot Data

(b) Sample Autocorrelations